Probability of EMC Failure and Sensitivity Analysis With Regard to Uncertain Variables by Reliability Methods

Mourad Larbi, Philippe Besnier, Bernard Pecqueux

Probability of EMC Failure and Sensitivity Analysis with regard to Uncertain Variables by Reliability Methods

Mourad Larbi, Philippe Besnier, *Senior Member, IEEE* and Bernard Pecqueux

***Abstract*— In this work, we use a statistical approach to treat a risk analysis of an EMC default. This approach relies upon reliability methods from probabilistic engineering mechanics. An estimation of a probability of failure (*i.e.* probability that the induced current by crosstalk causes a malfunction of a device connected at the end of a cable) and a sensitivity analysis of this probability of failure is carried out by taking into account uncertainties on input parameters. The reliability methods introduced in this work allow to compute a probability of failure with a relative low computational cost compared to Monte Carlo simulation.**

***Index Terms*— Electromagnetic susceptibility, transmission line, uncertainty propagation, reliability problem, failure probability, sensitivity analysis.**

I. Introduction

Since few years, many statistical approaches have been introduced in EMC[1]. It becomes a rather natural approach when dealing with physical phenomena that depends on numerous uncertain variables conditioning the interference levels. The development of these statistical techniques in the EMC area allowed for example to estimate the expectation and the standard deviation of an interest response depending on various random variables [1]–[3].

Only few approaches deal with estimation of extreme values in EMC [4]. However, it is a very relevant way to look at risk analysis. A typical case would be a detection of malfunction of a device connected to a wire end when illuminated by an electromagnetic field [5].

Moreover, such a device may differ from one to another due to manufacturing conditions. In this case, a set of devices would be ideally represented by a probability density function (pdf) of failure with regard to, for instance, the level of current applied to its input. Thus, a reliability analysis of an EMC system has to take into account the probability that the interfering current reaches a certain value and the probability of having a device failure for the specific current magnitude.

In this paper, we will first introduce the reliability analysis tools (from the probabilistic mechanics [6], [7]) allowing to estimate a *failure probability* denoted P_f defined as the probability of exceeding a certain threshold value. We will then provide factors indicating the sensitivity of this failure probability with respect to input parameters of the physical phenomenon. In Section III, we will apply these tools to analyse the risk of an EMC default by taking into account the uncertainty on input parameters influencing levels of interference for a simple example of crosstalk in a two wire transmission line.

This work was done during the Ph.D. thesis of M. Larbi supported by CEA, DAM, GRAMAT for the benefit of the Direction Générale de l'Armement-Unité de Management Nucléaire, Biologique et Chimique (DGA-UM NBC).

M. Larbi is with the Institute of Electronics and Telecommunications of Rennes (IETR), UMR CNRS 6164, INSA of Rennes, Rennes 35043, France, and CEA, DAM, GRAMAT, F-46500, Gramat, France, mail: mourad.larbi@insa-rennes.fr.

P. Besnier is with IETR, UMR CNRS 6164, INSA of Rennes, Rennes 35043, France, mail: philippe.besnier@insa-rennes.fr.

B. Pecqueux is with CEA, DAM, GRAMAT, F-46500, Gramat, France, mail: bernard.pecqueux@cea.fr.

[1]ElectroMagnetic Compatibility

II. Methods for reliability analysis

Due to the lack of knowledge regarding the input parameters of a set of equations, the analyst is constrained by using a statistical modelling by means of random variables describing the available information on the distribution of input parameters. Thus, the response of a numerical model (*i.e.* representing a physical phenomenon) becomes also uncertain. The purpose of *reliability analysis* consists in determining the probability of failure of a system and in providing a hierarchization of the input parameters (*sensitivity analysis*). This is based on the definition of a *limit state function* that is now introduced [8].

A. The limit state function

Let a random vector $\boldsymbol{X}$ of size M (containing M random variables, possibly correlated) describing the uncertainties identified in model inputs. The assessment of the reliability of a system relies on a limit state function g depending on vector of input parameters $\boldsymbol{X}$ defined as:

$$\begin{aligned} g : \mathbb{R}^M &\longrightarrow \mathbb{R} \\ \boldsymbol{X} &\longrightarrow y_S - \mathcal{M}(\boldsymbol{X}), \end{aligned} \tag{1}$$

where $\mathcal{M}$ is the numerical simulation model used and y_S is a determined threshold. The limit state function g is formulated as:

- $D_f = \{\boldsymbol{x};\ g(\boldsymbol{x}) \leq 0\}$ defines the *failure domain* of the system;
- $D_s = \{\boldsymbol{x};\ g(\boldsymbol{x}) > 0\}$ defines the *safe domain*;
- $\partial D = \{\boldsymbol{x};\ g(\boldsymbol{x}) = 0\}$ is the *limit state surface*.

We denote now by $f_{\boldsymbol{X}}$ the joint pdf of random vector $\boldsymbol{X}$, the probability of failure P_f of the system is then written:

$$P_f = \mathbb{P}(g(\boldsymbol{x}) \leq 0) = \int_{D_f} f_{\boldsymbol{X}}(\boldsymbol{x})\, \mathrm{d}\boldsymbol{x}. \tag{2}$$

In most cases, the integral defined in (2) has to be resolved by means of numerical methods such as Monte Carlo simulation (MCS). That requires numerous evaluations of the limit state function g, and of the numerical model $\mathcal{M}$. To overcome this limitation, approximation methods for reliability analysis [6] have been developed to compute the probability of failure at a relative low computational cost compared to MCS. These methods are based on the identification of the so-called *design point* which is now presented.

B. Transformation of the input variable space and identification of the design point

The principle of reliability methods is based on the transformation of the reliability problem from the physical space to the standard Gaussian space, in which reduced centered Gaussian variables are uncorrelated.

To identify the design point, the first step consists in rewriting the integral (2) in the standard Gaussian space by using an isoprobabilistic transformation $T : \boldsymbol{X} \longrightarrow \boldsymbol{\xi}$. Various transformations (e.g. Rosenblatt or Nataf transformation [6], [7]) have been proposed for the probabilistic transformation of physical input random variables. Rosenblatt transformation is applied when the joint probability distribution is known (a rich information but rarely available) while the Nataf transformation requires only the knowledge of marginal distributions of input variables and their correlations (a poor information but generally available). Once the Rosenblatt or Nataf transformation is applied, the obtained standard Gaussian random variables are transformed to *uncorrelated* standard Gaussian random variables [7]. Thus, (2) is reformulated in the uncorrelated Gaussian random variables space as follows:

$$P_f = \int_{g(T^{-1}(\boldsymbol{\xi}))\leq 0} \phi_M(\boldsymbol{\xi})\, \mathrm{d}\boldsymbol{\xi} = \int_{G(\boldsymbol{\xi})\leq 0} \phi_M(\boldsymbol{\xi})\, \mathrm{d}\xi_1 \ldots \mathrm{d}\xi_M, \tag{3}$$

where $G(\boldsymbol{\xi}) = g(T^{-1}(\boldsymbol{\xi}))$ and ϕ_M is the standard multinormal pdf. This pdf is maximal at the origin and decays exponentially with $\|\boldsymbol{\xi}\|^2$. Thus the points having the most significant contribution in the integral (3) are those of the failure domain that are the nearest to the origin of the standard Gaussian space.

The second step of the method is to identify the so-called design point $\boldsymbol{\xi}^*$ (or Most Probable Point (MPP) of failure), which is the point of the failure domain nearest to the origin in the standard Gaussian space. This point is the solution of a constrained optimization problem:

$$P^* = \boldsymbol{\xi}^* = \mathrm{Arg} \min_{\boldsymbol{\xi}\in\mathbb{R}^M} \left\{ \|\boldsymbol{\xi}\|^2 \ : \ G(\boldsymbol{\xi}) \leq 0 \right\}. \tag{4}$$

Various algorithms can be used to solve the optimization problem (4) such as the improved Hasofer-Lind-Rackwitz-Fiessler (iHLRF) algorithm given in [9]. Having found the design point $\boldsymbol{\xi}^*$, the so-called Hasofer-Lind reliability index β is defined as the distance of the design point to the origin in the standard Gaussian space:

$$\beta = \mathrm{sign}(G(\mathbf{0})) \cdot \|\boldsymbol{\xi}^*\|, \tag{5}$$

where $\mathrm{sign}(G(\mathbf{0}))$ is positive if $\mathbf{0}$ is in the safe domain and negative otherwise.

Once the design point is obtained, the third step is to perform Taylor series expansions of the limit state function at this point. These techniques are now presented.

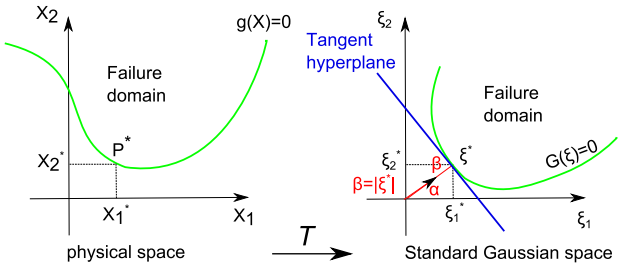

Fig. 1. Linearisation of the limit state function in FORM.

C. Computation of the failure probability from the design point

1) Principle of FORM and SORM approximations: The first order reliability method (FORM) performs a first-order Taylor series expansion of the limit state function G at the design point $\boldsymbol{\xi}^*$ for computing a *first order approximation of the failure probability*. This means to substitute the failure domain by the half space defined by a tangent hyperplane to the limit state surface at the design point $\boldsymbol{\xi}^*$ (Fig. 1). The equation of the hyperplane denoted by $\tilde{G}$ at the design point $\boldsymbol{\xi}^*$ may be researched as [8]:

$$\begin{aligned} \tilde{G}(\boldsymbol{\xi}) &= G(\boldsymbol{\xi}^*) + \nabla G(\boldsymbol{\xi}^*)^T \cdot (\boldsymbol{\xi} - \boldsymbol{\xi}^*) \\ &= \frac{\nabla G(\boldsymbol{\xi}^*)^T}{\|\nabla G(\boldsymbol{\xi}^*)\|} \cdot (\boldsymbol{\xi} - \boldsymbol{\xi}^*) = -\boldsymbol{\alpha}^T \cdot (\boldsymbol{\xi} - \boldsymbol{\xi}^*) \\ &= \beta - \boldsymbol{\alpha}^T \cdot \boldsymbol{\xi} = 0, \end{aligned} \tag{6}$$

where $(.)^T$ denotes the transposition, and the components of the unit vector $\boldsymbol{\alpha} = -\dfrac{\nabla G(\boldsymbol{\xi}^*)}{\|\nabla G(\boldsymbol{\xi}^*)\|}$ are the direction cosines of the gradient vector at the design point. Moreover, (6) has been obtained from $G(\boldsymbol{\xi}^*) = 0$ since $\boldsymbol{\xi}^*$ is on the limit state surface ∂D and normalizing the limit state function by $\|\nabla G(\boldsymbol{\xi}^*)\|$.

Thus, the first order approximation of P_f is written as [8]:

$$P_f = \int_{G(\boldsymbol{\xi})\leq 0} \phi_M(\boldsymbol{\xi})\, \mathrm{d}\boldsymbol{\xi} \approx \int_{Hyp(\boldsymbol{\xi}^*)} \phi_M(\boldsymbol{\xi})\, \mathrm{d}\xi_1 \ldots \mathrm{d}\xi_M. \tag{7}$$

Starting from the premise that the Gaussian random variables are uncorrelated, it is possible to demonstrate that (7) is given by [6], [7]:

$$P_f \approx P_{f,\mathrm{FORM}} = \Phi(-\beta), \tag{8}$$

where Φ is the cumulative distribution function (CDF) of a unidimensional standard Gaussian random variable.

However, the approximation (7) may sometimes be insufficient. Thus, the so-called second order reliability methods (SORM) have been proposed to provide a *second order approximation of the probability of failure*. It consists in replacing the limit state surface by a quadratic surface around the design point $\boldsymbol{\xi}^*$. Two types of SORM approximations are generally used: the so-called *curvature-fitting* SORM [10] and the *point-fitting* SORM [11]. In this paper, we only present the *curvature-fitting* SORM but the reader can refer to [11] for a review of point-fitting SORM. The idea of curvature-fitting SORM is based on the computation of the Hessian matrix of the limit state function at the design point $\boldsymbol{\xi}^*$. After using a rotation of the coordinate system in the standard Gaussian space (*i.e.* $\boldsymbol{v} = R \cdot \boldsymbol{\xi}$), the limit state function may be rewritten as [8]:

$$G(\boldsymbol{\xi}) \approx \beta - v_M + \sum_{i=1}^{M-1} \frac{1}{2}\kappa_i v_i^2, \tag{9}$$

where $\{\kappa_i, i = 1, \ldots, M-1\}$ stand for the curvature of the approximate paraboloïd around the design point. [10] has proposed the first formula to express the second order approximation of the probability of failure, but [12] improved it by the following:

$$P_f \approx P_{f,\text{SORM}} = \Phi(-\beta) \prod_{i=1}^{M-1} \frac{1}{\sqrt{1 - \dfrac{\phi(\beta)}{\Phi(-\beta)}\kappa_i}}. \tag{10}$$

The SORM approximation of the probability of failure in (10) proposes to correct the term obtained by FORM approximation in (8).

2) Importance sampling: The FORM-SORM approximations of the probability of failure P_f are obtained at a low computational cost compared to MCS. Otherwise, several drawbacks can be encountered when dealing with complex problems such as:

- the design point $\boldsymbol{\xi}^*$ found after solving the optimization problem (4) may have been incorrectly identified (*i.e.* $\boldsymbol{\xi}^*$ is a local minima instead of being a global minima);
- the quality of approximations of the probability of failure in (8) and (10) may not be sufficient.

To get over these limitations, a complementary approach called *importance sampling* (IS) has been introduced [13]. Since the weight of P_f is mainly localized around the design point $\boldsymbol{\xi}^*$, the method consists in concentrating the sampling around this point (Fig. 2) by selecting an importance sampling density (ISD) ψ [7]. In practice, ψ can be selected as a M-dimensional reduced Gaussian density function centered around the design point $\boldsymbol{\xi}^*$, *i.e.* $\psi(\boldsymbol{\xi}) = \phi_M(\boldsymbol{\xi} - \boldsymbol{\xi}^*)$. As shown in Appendix, this method provides an estimation of the probability of failure.

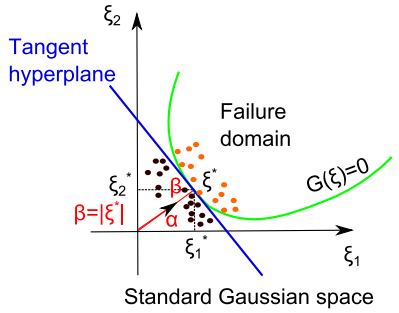

Fig. 2. Sampling concentrated around the design point $\boldsymbol{\xi}^*$.

D. Measurement of local sensitivity

Further information called *importance factors* may be derived from FORM analysis introduced in Section II-C.1. Their interest is to determine the weight of each input random variable of the physical model on the probability of failure. We therefore are interested by the influence of each random variable on the failure of the system, measured by the reliability index β at the design point $\boldsymbol{\xi}^*$.

1) Sensitivity of the reliability index to the variables: Starting from the linearised limit state function $\tilde{G}$ computed by FORM in (6), we notice that the direction cosines of $\boldsymbol{\alpha}$ represent the sensitivity of the reliability index β to the independent standard Gaussian variables as:

$$\boldsymbol{\alpha} = \left.\frac{\partial \beta}{\partial \boldsymbol{\xi}}\right|_{\boldsymbol{\xi}^*}. \tag{11}$$

Otherwise, the variance of the linearised limit state function $\tilde{G}$ is defined by:

$$\text{Var}\left[\tilde{G}\right] = \boldsymbol{\alpha}^T \cdot \text{Cov}\left[\boldsymbol{\xi}, \boldsymbol{\xi}\right] \cdot \boldsymbol{\alpha}, \tag{12}$$

since the standard Gaussian variables are independent. Using the fact that $\text{Cov}\left[\boldsymbol{\xi}, \boldsymbol{\xi}\right] = \text{Var}\left[\boldsymbol{\xi}\right] = I_M$, where I_M is the identity matrix of size M, and since $\boldsymbol{\alpha}$ is a unit vector, the variance of $\tilde{G}$ becomes:

$$\text{Var}\left[\tilde{G}\right] = \sum_{i=1}^{M} \alpha_i^2 = 1. \tag{13}$$

This means that the importance factors α_i^2 represents the proportion of the variance associated to the variable ξ_i. When the physical input random variables $\boldsymbol{X}$ are independent, each physical variable X_i is associated to each standard Gaussian variable ξ_i. In this case, the coefficients α_i^2 directly provide a measure of importance of each physical input random variable X_i. When the physical input random variables are correlated, the importance vector γ using the Jacobian of the probabilistic transformation T has to be introduced [7].

2) Sensitivity of the reliability index to the distribution parameters: Besides the sensitivity of the reliability index β to each random variable, the sensitivity of β to the distribution parameters (expectation, standard deviation, ...) can be derived. However, the obtained sensitivities by deriving β with respect to the distribution parameters do not enable an importance comparison between different

distribution parameters. In order to bypass this problem, a normalisation of sensitivities is carried out to get the *elasticities* of parameters defined by:

$$\epsilon_{p_{i_\lambda}} = \frac{p_{i_\lambda}}{\beta} \frac{\partial \beta}{\partial p_{i_\lambda}}\bigg|_{\boldsymbol{\xi}^*}, \tag{14}$$

where p_{i_λ} is the λ-th distribution parameter of the variable $X_i,\ i = 1, \ldots, M$. Note that once again, when the physical input random variables $X_i,\ i = 1, \ldots, M$ are correlated, the Jacobian matrix of the probabilistic transformation T must be introduced for computing the elasticities of parameters (see [7] for further details).

E. Computation of the failure probability in large dimensions

1) Subset simulation: In the reliability analysis, FORM, SORM and IS are classic tools allowing the engineer to solve the problem most of the time [8]. However, although these techniques are relatively robust, when the complexity of the problem increases (with for example a large number of the uncertain input parameter) the construction of a good ISD may be problematic [14]. Therefore, a new simulation method called subset simulation (SS) has been developed in [14] for estimating small failure probabilities in high dimensions.

Supposing that the failure event D_f is rare, the approach introduced in [14] consists in estimating the failure probability P_f by introducing more frequent intermediate conditional failure events $D_{f_i},\ i = 1, \ldots, R$ called subsets defined as $D_{f_1} \supset D_{f_2} \supset \ldots \supset D_{f_R} = D_f$. The several intermediate subsets are defined by $D_{f_i} = \{g(\boldsymbol{x}) \leq t_i,\ i = 1, \ldots, R\}$ where the set of thresholds $\{t_i,\ i = 1, \ldots, R\}$ is a decreasing sequence with $t_R = 0$. Thus, the failure probability P_f is given by definition of conditional probability as follows:

$$\begin{aligned} P_f &= \mathbb{P}(D_f) = \mathbb{P}(D_{f_R}) = \mathbb{P}\left(\bigcap_{i=1}^{R} D_{f_i}\right) \\ &= \mathbb{P}\left(D_{f_R} \mid D_{f_{R-1}}\right) \cdot \mathbb{P}\left(\bigcap_{i=1}^{R-1} D_{f_i}\right) \\ &= \ldots = \mathbb{P}(D_{f_1}) \prod_{i=2}^{R} \mathbb{P}\left(D_{f_i} \mid D_{f_{i-1}}\right). \end{aligned} \tag{15}$$

The principle of the SS is to estimate the probability of failure P_f by estimating the quantities $\mathbb{P}(D_{f_1})$ and the conditional probabilities $\{\mathbb{P}\left(D_{f_i} \mid D_{f_{i-1}}\right),\ i = 2, \ldots, R\}$ [14]. The estimation of these quantities depends in practice on the several subsets $D_{f_i},\ i = 1, \ldots, R$ and their associated thresholds t_i. The intermediate thresholds $\{t_i,\ i = 1, \ldots, R\}$ should be chosen in order to get intermediate conditional failure probabilities that are not too small to be well estimated. A target probability value P_f^c has to be chosen in practice (generally $P_f^c \approx 0.1 - 0.2$ [14]). The estimation of the first threshold t_1 is carried out by MCS where $\mathbb{P}(D_{f_1}) = P_f^c$. The following thresholds $\{t_i,\ i = 2, \ldots, R\}$ associated to the conditional failure events $\{D_{f_i} \mid D_{f_{i-1}}\},\ i = 2, \ldots, R$ are generated by Markov Chains Monte Carlo (MCMC) based on a modified Metropolis-Hastings (MMH) algorithm [14]. This technique is carried out until a negative threshold is obtained. Once that step is achieved, this means that the searched limit state surface $\{g(\boldsymbol{x}) = 0\}$ has been found (*i.e.* this is the R-step and the negative threshold t_R takes the value 0). Finally the last conditional failure probability $\{\mathbb{P}\left(D_{f_R} \mid D_{f_{R-1}}\right)\}$ is estimated [14].

In the next section, we propose to use these reliability analysis tools in the context of a simple crosstalk problem in transmission lines.

III. Computation and sensitivity analysis of the failure probability in a crosstalk problem

The results given in this section have been obtained by the open-source toolbox FERUM 4.1 [15] (Finite Element Reliability Using Matlab®), coupled to a computer code based on the transmission line theory using the BLT[2] equation formalism.

A. Presentation of the crosstalk configuration under study

In order to study the impact of uncertainties of input parameters on electromagnetic interferences, we examined an example of a two-wire lossless transmission line above a PEC[3] (Fig. 3). The two wires have the same length denoted Lg. Wire n°1 is located at a height denoted h_1 above the PEC being fed by an electromotive force $e = 1$ V. Two loads denoted R_1 and R_2 are connected at the ends of this wire. Wire n°2 is placed at a height denoted h_2 above the PEC and is loaded by two resistances denoted R_3 and R_4. We are interested in computing the induced current at the opposite end of the wire n°2, denoted $I_2(Lg)$. It depends on the following random variables:

- R_1 is a variable uniformly distributed between 1 Ω and 10 Ω;
- R_2 and R_3 are variables uniformly distributed between 10 kΩ and 100 kΩ;
- h_1 and h_2 are uniform random variables between 1.5 cm and 2.5 cm and vary independently from each other;
- Lg of the two-wire cable is a uniform random variable between 9.5 m and 10.5 m.

Furthermore, R_4 is set to 10 Ω, the distance d between the two wires is set to 1 cm and the diameter of each wire d_m is 1 mm. The objective of the study is to estimate a probability of failure P_f defined as the probability that the maximum of the induced current evaluated in a predefined frequency band Δ_f exceeds a threshold denoted I_t: $P_f = \mathbb{P}(\max_{\Delta f} I_2(Lg) \geqslant I_t)$.

In order to deal with extreme current values, we have chosen a frequency band for which wires are in resonance state. The interest of such case study is to adopt the point of view of an EMC engineer. At early design stage,

[2]Baum-Liu-Tesche
[3]Perfect Electric Conductor

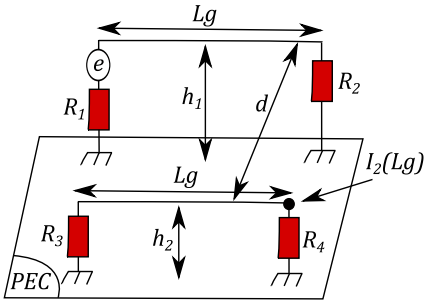

Fig. 3. Two wires above a PEC with the following uniform random variables: the loads R_1, R_2, R_3, the heights h_1, h_2 and the length Lg of the wires.

one has a modest information on the input parameters of the system such as cable positions or input impedances. However, it is necessary to ensure that $I_2(Lg)$ does not cause a malfunction of a device connected at the end of a cable. Otherwise, one is interested by the precautions to take on input parameters to avoid that the system fails.

B. Preliminary analysis of the performances of FORM

1) Illustration of FORM in a simple problem: To show the performances of a FORM analysis, the crosstalk problem presented in Section III-A has been simplified. Indeed, only resistances R_1 and R_2 (Fig. 3) have been considered as random variables in this simplified problem with the same probability distributions. All other random variables of the initial configuration are fixed to their mean values: $R_3 = 55$ kΩ, $h_1 = h_2 = 2$ cm and $Lg = 10$ m.

The aim of this simplified crosstalk problem is to highlight the good approximation of the failure probability P_f established by FORM and SORM which relies upon the approximation of the limit state function g. Thus, we have selected an arbitrarily fixed threshold $I_t = 73$ mA, and we computed $P_f = \mathbb{P}\left(\max_{\Delta f} I_2(Lg) \geqslant I_t\right)$ by FORM and SORM analysis. The failure probabilities $P_{f,\mathrm{FORM}}$ and $P_{f,\mathrm{SORM}}$ are then compared to a reference result obtained by 10,000 realizations from MCS, $P_{f,\mathrm{MCS}} = 0.049 \pm 4\%$. Note that 10,000 realizations were carried out to achieve a trade-off between computation time and accuracy of the estimation of P_f. Thus, the approximation of the failure probability obtained by FORM is $P_{f,\mathrm{FORM}} = 0.069$ using 106 calls to the computer code. To improve the precision of the result obtained by FORM, we use a SORM approximation which provides $P_{f,\mathrm{SORM}} = 0.049$ using 5 additional calls to the computer code. Note that SORM is carried out once the design point $\boldsymbol{\xi}^*$ was identified with FORM. We notice that the results provided by FORM and especially SORM are quite satisfactory in so far as there is a little difference between them and those obtained from a MCS with 10,000 realizations. In order to give a representation of the approximation of the failure probability P_f computed by FORM analysis, we represented 2,000 realizations of g with respect to the loads R_1 and R_2 in the physical space in Fig. 4(a) and in the Gaussian space in Fig. 4(b). An illustration of the approximation of the limit state function G by a tangent hyperplane at the design point $\boldsymbol{\xi}^*$ carried by FORM analysis in the Gaussian space is also shown in Fig. 4(b). Thus, we see that the tangent hyperplane (in black) established by FORM at the design point $\boldsymbol{\xi}^*$ (in green) separates the realizations of the limit state function G which are in the failure domain (in magenta) and those in the safe domain (in blue). The red realization in Fig. 4(a) is the mean of the random vector $\boldsymbol{X} = \{R_1, R_2\}^T$ in the physical space which is transformed to the origin of the Gaussian space in Fig. 4(b).

2) Illustration of FORM in the crosstalk configuration under study: As shown above, FORM and SORM provide a good approximation of the failure probability P_f when the problem considered is very simple (*i.e.* with two input random variables). Let us go back to the initial configuration presented in Section III-A (with six input random variables). First, it is interesting to observe the behaviour of the induced current $I_2(Lg)$ in resonance regime. Thus, a representation of the induced current $I_2(Lg)$ in the frequency band [5-10 MHz] has been given by 10 realizations from MCS in Fig. 5. We observe an important variability of $I_2(Lg)$ by means of resonance phenomena which appear around frequencies f_n such as $f_n = (2n+1)\cdot c/4\cdot Lg$, where $n \in \mathbb{N}$, Lg is the length of the line and c is the speed of light. The first frequency resonant of the line is 7.5 MHz. However, a particular pattern of the curve is observed due to the combination of inductive and capacitive coupling.

We want now to approximate the failure probability P_f by FORM analysis with a threshold value $I_t = 70$ mA. Thus, the failure probability obtained by FORM is $P_{f,\mathrm{FORM}} = 0.139$ with 142 calls to the computer code. In a second time, an approximation by SORM analysis indicates $P_{f,\mathrm{SORM}} = 0.082$ with 27 additional calls to the computer code. The reference result, obtained by 10,000 realizations from MCS is $P_{f,\mathrm{MCS}} = 0.087 \pm 3\%$. In this case, we notice a significant gap between the result provided by FORM and the reference result. This shows the limitations of FORM analysis when the complexity of the problem increases. In order to show again the approximation of the limit state function g carried out by FORM, 2,000 evaluations of the limit state function g from MCS are represented on the axis of the random load R_1 in the physical space in Fig. 6(a). After using the probabilistic transformation (from physical space to Gaussian space), FORM performs an approximation of the surface state limit by a tangent hyperplane (in black) at the design point $\boldsymbol{\xi}^*$ (in green) in Fig. 6(b). In this case, we see for example on the axis of the Gaussian random variable ξ_1 that the realizations of g in the safe domain (in blue) and those in the failure domain (in magenta) are not very well separated. This allows to highlight the limitations of the FORM analysis that may poorly approximate the failure domain. This is due to the limit state function g which has a non-linear and too irregular shape in the frequency band [5-10 MHz]. Moreover, the approximation of the limit state function g established by SORM was sufficient in this case. However, if the number

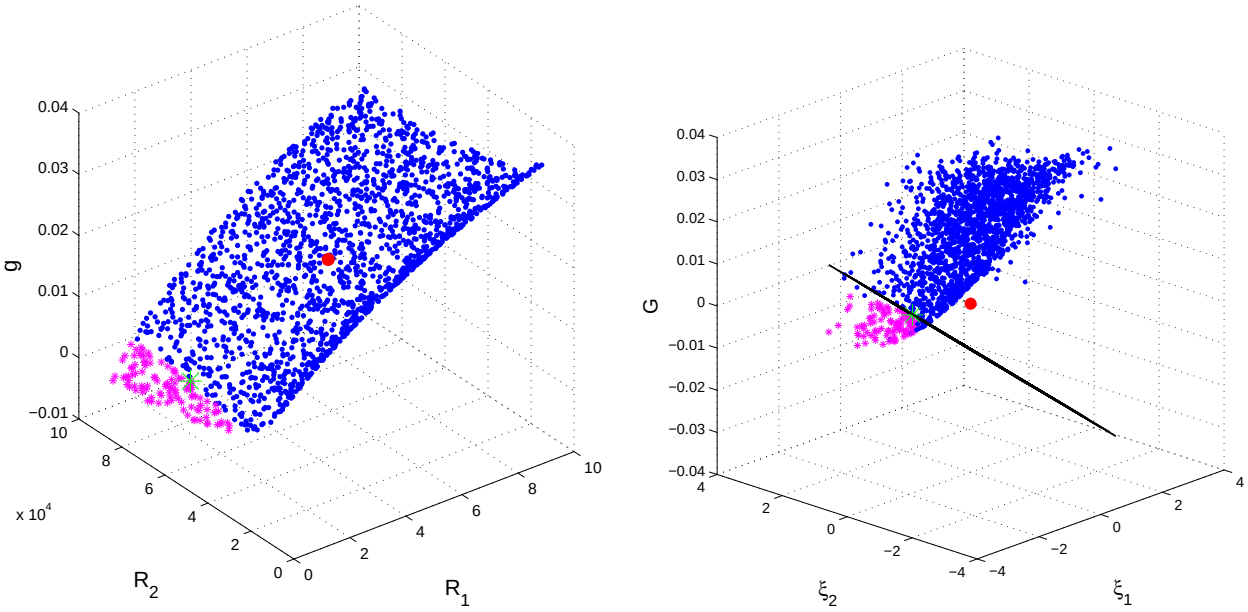

(a) (b)

Fig. 4. Representation of the limit state function g with respect to the random vector $\boldsymbol{X} = \{R_1, R_2\}^T$ in the physical space (a) and in the Gaussian space (b) obtained by 2,000 realizations from MCS. Realizations in the safe domain are in blue and those in the failure domain are in magenta. The red realization is the evaluation of g for the variables mean value and the green realization is the design point $\boldsymbol{\xi}^*$ at which the FORM hyperplane (in black) is determined.

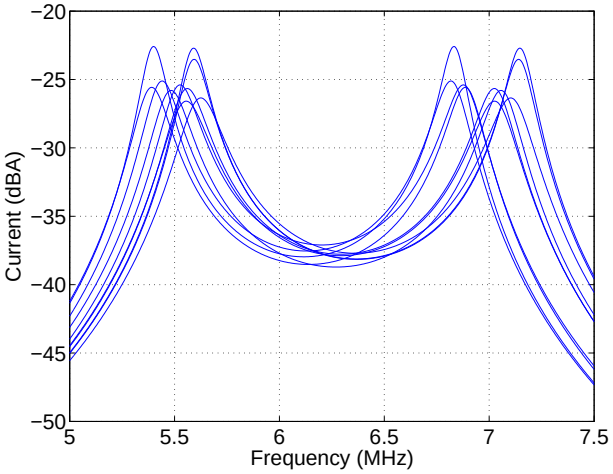

Fig. 5. Representation of the induced current $I_2(Lg)$ with respect to the frequency band [5-10 MHz] given by 10 realizations from MCS depending on the uniform random variables: the loads R_1, R_2, R_3, the heights h_1, h_2 and the length Lg of the wires.

of input random variables increases again, SORM could also be insufficient to approximate the failure probability P_f. In order to overcome possible difficulties of FORM and SORM, the approaches by IS and SS introduced in Sections II-C.2 and II-E.1, which are more robust with regard to the complexity of the problem, will be used in the following analysis.

C. Susceptibility of a device connected to wire n°2

The first part of Section III was devoted to the estimation of extreme values probability of the induced current $I_2(Lg)$. However, an EMC engineer aims at estimating the probability of having an immunity problem of the connected device whose input impedance is R_4. A failure pdf of the device is supposed to be known. The following part describes a procedure to compute the probability of having a failure for the device.

1) Integration of failure device in the crosstalk problem: In the crosstalk study considered, rather than choosing the load R_4 as a random variable, we fixed R_4 to 10 Ω. Indeed, R_4 has been chosen in this way to represent a set of devices (having a known impedance) manufactured under the same conditions and connected at the end of a cable. Since each device may differ from each other owing to manufacturing conditions, each of them has its own probability of failure and therefore the set of devices can be represented by a failure pdf (provided from experiments or theoretical analysis).

Starting from the knowledge of the failure probability of the device, the purpose of the study becomes now to estimate the probability of failure $P_{f,\text{sys}}$ of a system defined as: *the probability of having a device failure D_{f_d} if the maximum of the induced current computed in the frequency band Δf = [5-10 MHz] reaches this threshold value.* In terms of probabilities, this means to estimate the following quantity:

$$P_{f,\text{sys}} = \mathbb{P}\left(D_{f_d} | \max_{\Delta f} I_2(Lg)\right) \cdot \mathbb{P}\left(\max_{\Delta f} I_2(Lg)\right), \quad (16)$$

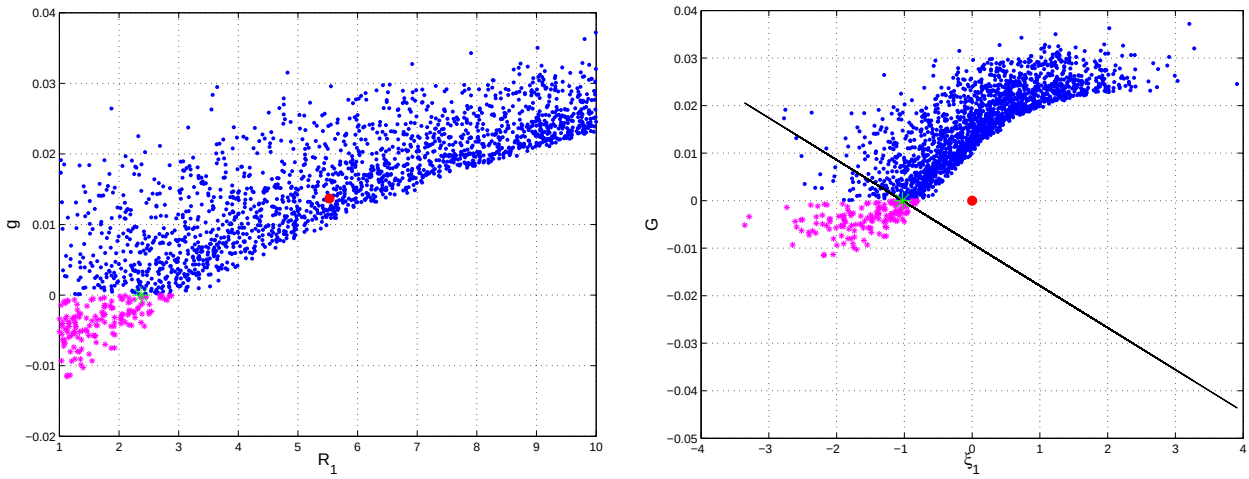

(a) (b)

Fig. 6. (a) Evaluation of the limit state function g with respect to the component random variable R_1 (among the six random variables) in the physical space (a) and in the space of the corresponding Gaussian random variable (b) obtained by 2,000 realizations from MCS. Realizations in the safe domain are in blue and those in the failure domain are in magenta. The red realization is the evaluation of g for the mean value of R_1 and the green realization is the component ξ_1^* of the design point $\boldsymbol{\xi}^*$ at which the FORM hyperplane (in black) is determined.

where $\mathbb{P}\left(D_{f_d}|\max_{\Delta f} I_2(Lg)\right)$ denotes the conditional probability of D_{f_d} given $\max_{\Delta f} I_2(Lg)$.

For the only purpose of illustration, an histogram of $\max_{\Delta f} I_2(Lg)$ has been built up from 10,000 realizations from MCS. It is shown in blue in Fig. 7. The probability of having a device failure $\mathbb{P}\left(D_{f_d}\right)$ is supposed to follow a Gaussian distribution with a mean of 80 mA and a standard deviation of 6 mA. The corresponding pdf appears in red in Fig. 7. Two cases may occur. In the first case, no intersection takes place between the upper values of the histogram of $\max_{\Delta f} I_2(Lg)$ and the lower values of currents for which $\mathbb{P}\left(D_{f_d}\right)$ is significant. In this case, $P_{f,\text{sys}}$ may be considered to be zero and the device is reliable with a very high level of probability. Curves of Fig. 7 figure out the opposite situation. Since the two curves overlap, $P_{f,\text{sys}}$ given by (16) will be significantly different from zero.

2) Computation of the failure probability of the EMC system: The failure probability $P_{f,\text{sys}}$ of the EMC system is computed in discretizing the device failure domain (the filled area under the failure pdf) as:

$$P_{f,\text{sys}} \approx \sum_{i=1}^{N} \Big[\mathbb{P}(D_{f_d}|\max_{\Delta f} I_2(Lg)) \in [I_{2_{\min}} + (i-1)\cdot\Delta_i, I_{2_{\min}} + i\cdot\Delta_i]\Big] \cdot \Big[\mathbb{P}(\max_{\Delta f} I_2(Lg) \geq I_{2_{\min}} + i\cdot\Delta_i) - \mathbb{P}(\max_{\Delta f} I_2(Lg) \geq I_{2_{\min}} + (i-1)\cdot\Delta_i)\Big]. \quad (17)$$

$I_{2_{\min}}$ corresponds to the lower limit of the current below which $\mathbb{P}\left(D_{f_d}\right)$ is negligible. We select $I_{2_{\min}}$ to be about three times the standard deviation below the mean, *i.e.* $I_{2_{\min}} = 60$ mA. The step Δ_i is chosen to be slightly below the standard deviation, as a trade-off between computation time and accuracy of estimation of $P_{f,\text{sys}}$. The summation is stopped at N discrete intervals for which $\mathbb{P}(\max_{\Delta f} I_2(Lg) \geq I_{2_{\min}} + N\cdot\Delta_i)$ is negligible. For N intervals, one needs $(N+1)$ estimation of $\mathbb{P}(\max_{\Delta f} I_2(Lg))$ with FORM, SORM, IS or SS. Namely in the case of Fig. 7, $N = 4$ intervals are selected with $I_{2_{\min}} = 60$ mA, $\Delta_i = 5$ mA. Thus, the upper evaluation is done for $I_2(Lg) = 80$ mA, for which the probability to exceed such a value has been found negligible, *e.g.* $7.9\cdot10^{-4} \pm 71\%$ by SS.

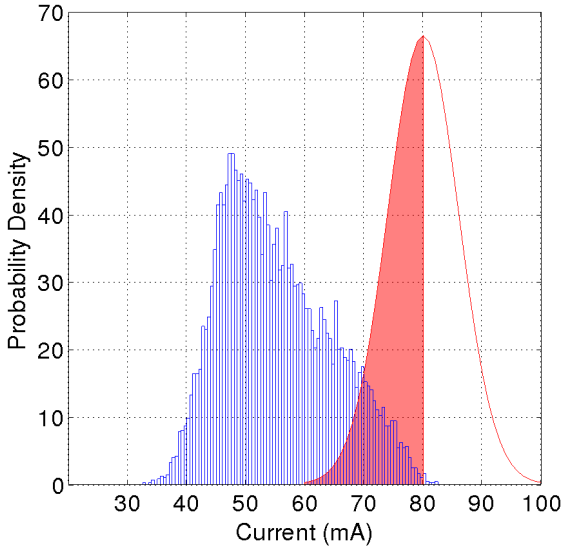

Fig. 7. Histogram of the maximum induced current $I_2(Lg)$ in the frequency band [5 – 10 MHz] (blue color) and Gaussian pdf of the device failure R_4 (red color). The filled area under the Gaussian pdf is the failure probability $P_{f,\text{sys}}$ of the system. R_1 is uniformly distributed between 1 Ω and 10 Ω.

The failure probability $P_{f,\text{sys}}$ computed by FORM, SORM, IS and SS as well as their number of calls to the model n_{sys} are listed in Table I. The total failure

TABLE I
COMPARISON OF RELIABILITY METHODS IN [5-10 MHz] WHEN R_1 IS UNIFORMLY DISTRIBUTED BETWEEN 1 Ω AND 10 Ω

	FORM	SORM	IS	SS	MCS
$P_{f,\text{sys}}$ (%)	3.26	1.97	[1.67 - 2.11]	[1.66 - 2.36]	[2.00 - 2.19]
n_{sys}	1113	135[a]	1100	1800	10000

[a] in addition to FORM.

probability of the EMC system computed by FORM is around 3.2% while those computed by SORM, IS and SS are around 2%. The number of calls to the model used by each method is respectively 1113, 135, 1100 and 1800. The results obtained are compared to the reference result obtained by 10,000 realizations from MCS, $P_{f,\text{sys,MCS}} = [2.00 - 2.19\%]$. We notice that the results provided by SORM, IS and SS are quite satisfactory as much as the difference between them and the reference result is very low. Numbers within brackets indicate the confidence interval determined from IS, SS and MCS estimations. On the other side, the reduction of the number of calls to the model is significant.

3) Sensitivity of the failure probability $P_{f,\text{sys}}$ of the EMC system: The failure probability $P_{f,\text{sys}}$ of the EMC system computed previously has been obtained around 2%. During the FORM analysis, we obtained the importance factors introduced in Section II-D.1. Thus, the importance factors on the failure probability for exceeding the threshold value $I_t = 60$ mA (*i.e.* the lowest current value for which the system begins to be faulty) are $R_1 = 95\%$, $R_2 = 2\%$ and $R_3 = 2\%$. Other input variables are negligible. This shows that the input variable that an EMC engineer has to control to avoid that the system fails is the load R_1. However, the importance factors do not give any information on the measures to be taken in order to avoid a possible failure of the system. In order to obtain this information, we need to exploit the elasticities of parameters introduced in Section II-D.2 thanks to FORM analysis for the threshold value $I_t = 60$ mA. A representation of elasticities of the lower bound (the upper bound could have been chosen but it was less influential) of each input variable defined by bar plots appears in Fig. 8. For example, an increase of lower bounds $R_{1_{\min}} = 1$ Ω of the load R_1 and $h_{1_{\min}} = 1.5$ cm of the height h_1 of the wire n°1 will cause a decrease of the failure probability $P_{f,\text{sys}}$ of the EMC system (here an increase of $R_{1_{\min}} = 1$ Ω will have more impact than $h_{1_{\min}} = 1.5$ cm since the bar plot is the largest). Inversely, an increase of lower bounds $R_{2_{\min}} = 10$ kΩ and $R_{3_{\min}} = 10$ kΩ will entail an increase of the failure probability $P_{f,\text{sys}}$ while the lower bounds $h_{2_{\min}} = 1.5$ cm (of the height h_2) and $Lg_{\min} = 9.5$ m (of the length Lg of the wires) are negligible. We now suppose that the system designer is able to specify a more restrictive lower bound for R_1, increasing it from 1 Ω to 2 Ω. We recompute, in the same way, the failure probability $P_{f,\text{sys}}$ with the same random variables than previously but now the load R_1 is uniformly distributed

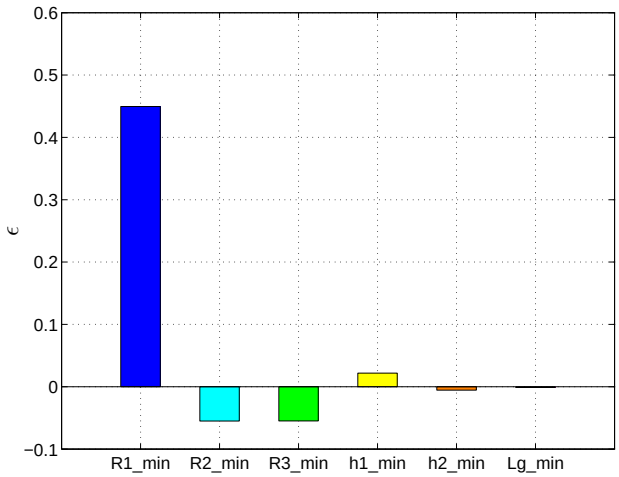

Fig. 8. Elasticities of the lower bound of each input random variable calculated by FORM analysis for the threshold value $I_t = 60$ mA.

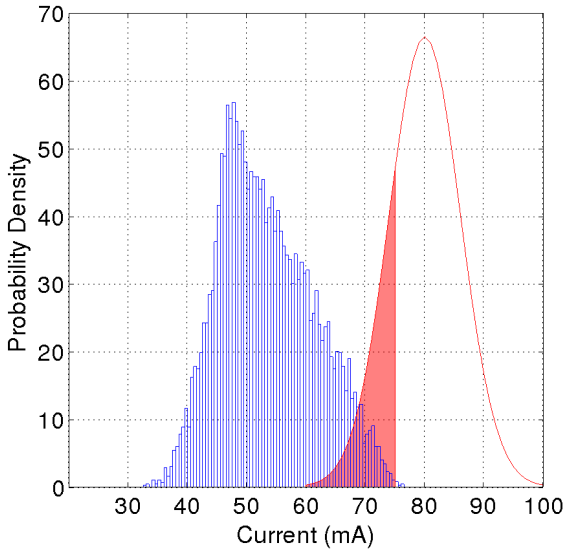

Fig. 9. Histogram of the maximum induced current $I_2(Lg)$ in the frequency band $[5 - 10$ MHz] (blue color) and Gaussian pdf of the device failure R_4 (red color). The filled area under the Gaussian pdf is the failure probability $P_{f,\text{sys}}$ of the system. R_1 is uniformly distributed between 2 Ω and 10 Ω.

between 2 Ω and 10 Ω. Once again, 10,000 evaluations of the maximum of the induced current $I_2(Lg)$ from MCS allowed to represent the failure probability $P_{f,\text{sys}}$ in Fig. 9. This failure probability $P_{f,\text{sys}}$ is represented by the filled area under the failure pdf of device. We notice that this filled area has been reduced compared to that of Fig. 7 (which corresponds to the case where $R_{1_{\min}} = 1$ Ω), we only need to use N=3 intervals.

The results of $P_{f,\text{sys}}$ obtained by reliability methods and their respective numbers of calls to the model n_{sys} are listed in Table II. The failure probability results to less than $P_{f,\text{sys}} = 1\%$ by reliability methods. Once again the results provided by SORM, IS and SS are close to the reference result obtained by 10,000 realizations from MCS. As an indication, the probability that the maximum of the

induced current $I_2(Lg)$ exceeds 60 mA switch from 30% when R_1 was uniformly distributed between 1 Ω and 10 Ω, to 22% when R_1 is uniformly distributed between 2 Ω and 10 Ω. This shows the impact of a slight modification of the load R_1.

TABLE II
COMPARISON OF RELIABILITY METHODS IN [5-10 MHz] WHEN R_1 IS UNIFORMLY DISTRIBUTED BETWEEN 2 Ω AND 10 Ω

	FORM	SORM	IS	SS	MCS
$P_{f,\text{sys}}$ (%)	1.36	0.74	[0.67 - 0.85]	[0.53 - 0.94]	[0.73 - 0.80]
n_{sys}	984	108[a]	900	1558	10000

[a] in addition to FORM.

IV. Conclusion

In this work, we have proposed various reliability methods allowing to compute a probability of failure in an EMC context, *i.e* the probability that the induced current exceeds a threshold value by taking into account uncertainties on input parameters of a numerical model.

These methods at a low computational cost compared to Monte Carlo simulation, estimate rather well the probability of failure when we treat a simple problem (*e.g.* with two input random variables). However, when the problem becomes more complex with an increasing of the number of input random variables, classic methods such as FORM and SORM can fail in estimating a probability of failure (even if in this work, SORM still provided good approximations of the failure probability). This leads to use more efficient methods such as importance sampling (IS) and subset simulation (SS).

These tools of reliability analysis enable a quick estimation of risks starting from "vague" information on input parameters such as cable positions or input impedances, which is believed to be useful for EMC engineers.

Given the knowledge of the probability of failure of a device, we may provide the solution of the estimation problem of the risk of failure for the device, once the probability of exceeding current thresholds at its input is determined through reliability methods. Choosing a simple crosstalk problem enables performing Monte Carlo simulations with relatively low cost computations in order to provide reference results. The advantage of reliability methods should be more pronounced for more complex problems with high dimensions. This extension is the object of further work.

Acknowledgment

This work was supported by the French Alternative Energies and Atomic Energy Commission-Military Applications Division, (CEA, DAM, GRAMAT) through studies for the benefit of DGA/UM NBC.

Appendix
Probability of Failure Estimated from the Importance Sampling Technique

The probability of failure P_f can be rewritten as:

$$\begin{aligned} P_f &= \int_{\mathbb{R}^M} \mathbb{1}_{D_f} \phi_M(\boldsymbol{\xi})\, \mathrm{d}\boldsymbol{\xi} \\ &= \int_{\mathbb{R}^M} \mathbb{1}_{D_f} \frac{\phi_M(\boldsymbol{\xi})}{\psi(\boldsymbol{\xi})} \psi(\boldsymbol{\xi})\, \mathrm{d}\boldsymbol{\xi}, \end{aligned} \tag{18}$$

where $\mathbb{1}_{D_f}$ is the indicator function of the failure domain taking the value 1 in the failure domain and 0 in the safe domain. The expression (18) can be reformulated as the expectation $\mathrm{E}_\psi[\cdot]$ with respect to the ISD ψ:

$$P_f = \mathrm{E}_\psi \left[\mathbb{1}_{D_f} \frac{\phi_M(\boldsymbol{\xi})}{\psi(\boldsymbol{\xi})} \right]. \tag{19}$$

An estimator of P_f is then provided by Monte Carlo simulation (see Fig. 2):

$$P_{f,\text{IS}} = \frac{1}{N} \sum_{k=1}^{N} \mathbb{1}_{D_f}^{(k)} \frac{\phi_M(\boldsymbol{\xi}^{(k)})}{\psi(\boldsymbol{\xi}^{(k)})}, \tag{20}$$

where the sample set $\{\boldsymbol{\xi}^{(k)}, k = 1, \ldots, N\}$ is now from the sampling density function ψ. It is also possible to provide an estimator of the variance of P_f:

$$\widehat{\mathrm{Var}}[P_{f,\text{IS}}] \approx \frac{1}{N-1} \left(\frac{1}{N} \sum_{k=1}^{N} \left(\mathbb{1}_{D_f}^{(k)} \left(\frac{\phi_M(\boldsymbol{\xi}^{(k)})}{\psi(\boldsymbol{\xi}^{(k)})} \right)^2 \right) - P_{f,\text{IS}}^2 \right). \tag{21}$$

References

[1] O. Sy, J. Vaessen, M. van Beurden, A. Tijhuis, and B. Michielsen, "Probabilistic study of the coupling between deterministic electromagnetic fields and a stochastic thin-wire over a pec plane," in *Electromagnetics in Advanced Applications, 2007. ICEAA 2007. International Conference on*, Torino, Italy, Sept. 2007.

[2] L. De Menezes, A. Ajayi, C. Christopoulos, P. Sewell, and G. Borges, "Efficient computation of stochastic electromagnetic problems using unscented transforms," *Science, Measurement Technology, IET*, vol. 2, no. 2, pp. 88–95, March 2008.

[3] M. Magdowski, S. Tkachenko, and R. Vick, "Coupling of stochastic electromagnetic fields to a transmission line in a reverberation chamber," *Electromagnetic Compatibility, IEEE Transactions on*, vol. 53, no. 2, pp. 308–317, May 2011.

[4] C. Kasmi, M. Hélier, M. Darces, and E. Prouff, "Modeling extreme values resulting from compromising electromagnetic emanations generated by an information system," *Comptes Rendus Physique*, Apr. 2014.

[5] E. Genender, A. Kreth, D. Zamow, H. Garbe, and S. Potthast, "Combination of the failure probability with a random angle of incidence of the radiated interference," in *General Assembly and Scientific Symposium, 2011 XXXth URSI*, Aug 2011, pp. 1–4.

[6] O. Ditlevsen and H. Madsen, *Structural reliability methods*. J. Wiley and Sons, Chichester, 1996.

[7] M. Lemaire, A. Chateauneuf, and J.-C. Mitteau, *Structural reliability*. J. Wiley and Sons, 2010.

[8] B. Sudret, *Uncertainty propagation and sensitivity analysis in mechanical models – Contributions to structural reliability and stochastic spectral methods*, Oct. 2007, habilitation à diriger des recherches, Université Blaise Pascal, Clermont-Ferrand, France.

[9] Y. Zhang and A. Der Kiureghian, "Two improved algorithms for reliability analysis," in *Reliability and Optimization of Structural Systems*. Springer, 1995, pp. 297–304.

[10] K. Breitung, "Asymptotic approximations for multinormal integrals," *Journal of Engineering Mechanics*, vol. 110, no. 3, pp. 357–366, Mar. 1984.
[11] A. Der Kiureghian, H.-Z. Lin, and S.-J. Hwang, "Second-order reliability approximations," *Journal of Engineering Mechanics*, vol. 113, no. 8, pp. 1208–1225, Aug. 1987.
[12] M. Hohenbichler, S. Gollwitzer, W. Kruse, and R. Rackwitz, "New light on first-and second-order reliability methods," *Structural Safety*, vol. 4, no. 4, pp. 267–284, 1987.
[13] R. Melchers, "Radial importance sampling for structural reliability," *Journal of Engineering Mechanics*, vol. 116, no. 1, pp. 189–203, Jan. 1990.
[14] S.-K. Au and J. Beck, "Estimation of small failure probabilities in high dimensions by subset simulation," *Probabilistic Engineering Mechanics*, vol. 16, no. 4, pp. 263–277, Oct. 2001.
[15] J.-M. Bourinet, C. Mattrand, and V. Dubourg, "A review of recent features and improvements added to ferum software," in *Proc. of the 10th International Conference on Structural Safety and Reliability (ICOSSAR'09)*, Osaka, Japan, Sept. 2009.

Mourad Larbi received the M.S. degree in engineering mathematics and applied economics from the University of Nice Sophia-Antipolis, Nice, France, in 2011. He is currently working toward the Ph.D. degree in electronics and telecommunications at CEA, DAM, Gramat and at the Institute of Electronics and Telecommunications of Rennes (IETR), INSA of Rennes, France. His research interests concern statistical analysis applied to the prediction of extreme electromagnetic events in the context of many uncertain parameters.

Philippe Besnier (M'04, SM'10) received the diplôme d'ingénieur degree from Ecole Universitaire d'Ingénieurs de Lille (EUDIL), Lille, France, in 1990 and the Ph.D. degree in electronics from the university of Lille in 1993.

Following a one year period at ONERA, Meudon as an assistant scientist in the EMC division, he was with the Laboratory of Radio Propagation and Electronics, University of Lille, as a researcher at the Centre National de la Recherche Scientifique (CNRS) from 1994 to 1997. From 1997 to 2002, Philippe Besnier was the Director of Centre d'Etudes et de Recherches en Protection Electromagnétique (CERPEM): a non-profit organization for research, expertise and training in EMC, and related activities, based in Laval, France. He co-founded TEKCEM in 1998, a private company specialized in turn-key systems for EMC measurements. Back to CNRS in 2002, he has been since then with the Institute of Electronics and Telecommunications of Rennes (IETR), Rennes, France. Philippe Besnier was appointed as senior researcher at CNRS in 2013 and has been co-head of the Antennas and Microwave devices departement of IETR since 2012. His research activities are mainly dedicated to interference analysis on cable harnesses (including electromagnetic topology), reverberation chambers, near-field probing and recently to the analysis of uncertainty propagation in EMC modelling.

Bernard Pecqueux was born in Amiens, France, in 1957. He received the M.S. degree in research physics in 1978 from the University of Amiens, France, and the Ph.D. degree in electromagnetics in 1982 from the University of Limoges, France. He joined DGA/CEG (Délégation Générale pour l'Armement/Centre d'Etudes de Gramat) in 1984 and CEA Gramat (Atomic Commission) in 2010 as a scientist. His current research interests include numerical modelling particularly in the time domain (FDTD, FETD) and coupling studies in the NEMP and HPM domains.